

pubs.acs.org/JACS Article

Active Site Dynamics in Molybdenum-Based Silica-Supported Olefin Metathesis Catalysts: Site Renewal and Decay Beyond the Chauvin Cycle

Ran Zhu, Griffin Drake, Husain H. Adamji, Zachariah J. Berkson, Jie Zhu, Ashley R. Head, Heather J. Kulik, Christophe Copéret, and Yuriy Román-Leshkov*



Cite This: https://doi.org/10.1021/jacs.5c15418



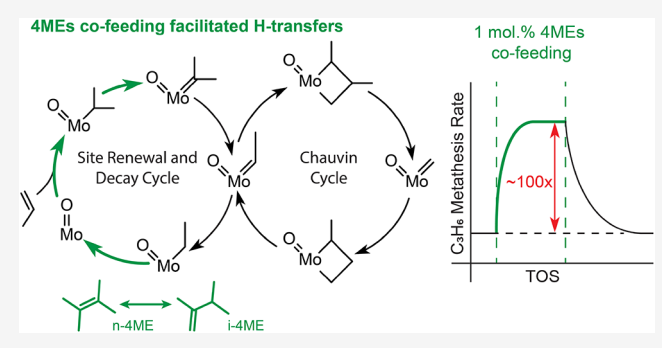
ACCESS I

III Metrics & More

Article Recommendations

Supporting Information

ABSTRACT: Heterogeneous olefin metathesis catalysts exhibit low active site densities and unpredictable kinetics due to dynamic active site formation and decay processes. Here, we establish a quantitative framework that captures active site generation, renewal, and decay in olefin metathesis over silica-supported molybdenum oxide catalysts, enabling a mechanistic explanation of catalytic behavior and strategies to achieve high, stable activity. Steady-state active site titrations reveal that 2,3-dimethyl-butene isomers (4MEs) cofeeding increases active site density by up to 4.3-fold, directly correlating with enhanced metathesis rates. Spectroscopic studies demonstrate that 4MEs facilitate Mo(VI) reduction to Mo(IV) and interact strongly with surface Si–OH



groups, generating labile protons that promote active site formation via a 1,2-proton shift mechanism. Kinetic modeling indicates that ethylene acts as a decay promoter, shifting kinetic control away from the Chauvin cycle and suppressing metathesis activity. Comparative studies on catalysts with varying Mo loading reveal that promotion is most effective for dispersed molybdate species, with a decline at higher Mo loadings. These findings provide a unified mechanistic framework for heterogeneous olefin metathesis, offering new strategies to enhance active site accessibility, mitigate deactivation, and optimize catalyst design.

INTRODUCTION

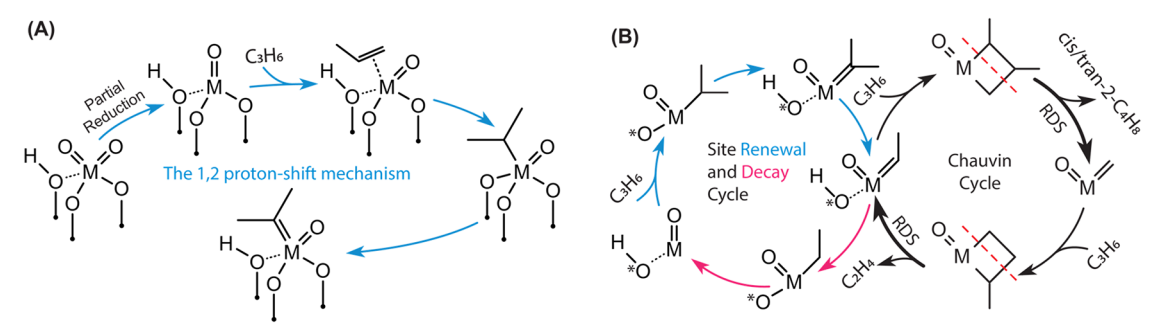
Olefin metathesis plays an important role in both industrial processes and fundamental research due to its high atomeconomy, minimal byproduct formation, and broad applicability from fine chemical synthesis to large-scale production of commodity chemicals.¹⁻³ While heterogeneous olefin metathesis is widely accepted to proceed via the Chauvin mechanism, involving metal alkylidene and metallacyclobutane intermediates, 4,5 the nature of the active sites remains uncertain, and direct spectroscopic detection of alkylidene species has proven challenging.^{6,7} The prevailing hypothesis suggests that active sites form in situ from isolated metal-oxo or metal-dioxo precursors upon olefin exposure at elevated temperatures. 4,8 However, the high kinetic and thermodynamic barriers associated with activation^{8,9} not only result in a low fraction of catalytically active metal centers but also make site formation highly dynamic and dependent on reaction conditions. The transient nature of active sites prevents direct quantification, complicating kinetic analyses and hindering rigorous comparisons between different catalyst formulations. Consequently, the lack of a predictive framework linking active site population, turnover, and deactivation pathways continues to limit the rational design of heterogeneous catalysts.^{4,9}

These limitations manifest as deviations from classical kinetic models, where heterogeneous systems exhibit higherthan-expected reaction orders and reactants such as ethylene act as rate-demoting species in cross-metathesis reactions. 10,11 To address this gap, we recently proposed that active sites in silica-supported tungsten oxides undergo a dynamic renewal and decay cycle alongside the Chauvin cycle, with site formation governed by a 1,2-proton shift mechanism involving proximal silanol groups. 12 In this framework, cofed substituted olefins, such as 2,3-dimethyl-1-butene (i-4ME), act as proton shuttles, accelerating site formation and increasing overall catalytic activity (Scheme 1A). 12-14 While this promotion strategy provided key mechanistic insights, a quantitative understanding of active site populations and their dependence on reaction conditions remained elusive. A key challenge lies in the intrinsic instability of metathesis active sites, which renders

Received: September 3, 2025 Revised: November 7, 2025 Accepted: November 7, 2025



Scheme 1. (A) 1,2-Proton Shift Mechanism on Partially Reduced Supported Metal (Mo or W) Oxides, and (B) Active Site Renewal and Decay Cycle Through 1,2-Proton Shift Mechanism, Where *O is a Lattice Oxygen of the Support and M is the Metal Center^a



^aRDS stands for rate-determining step.

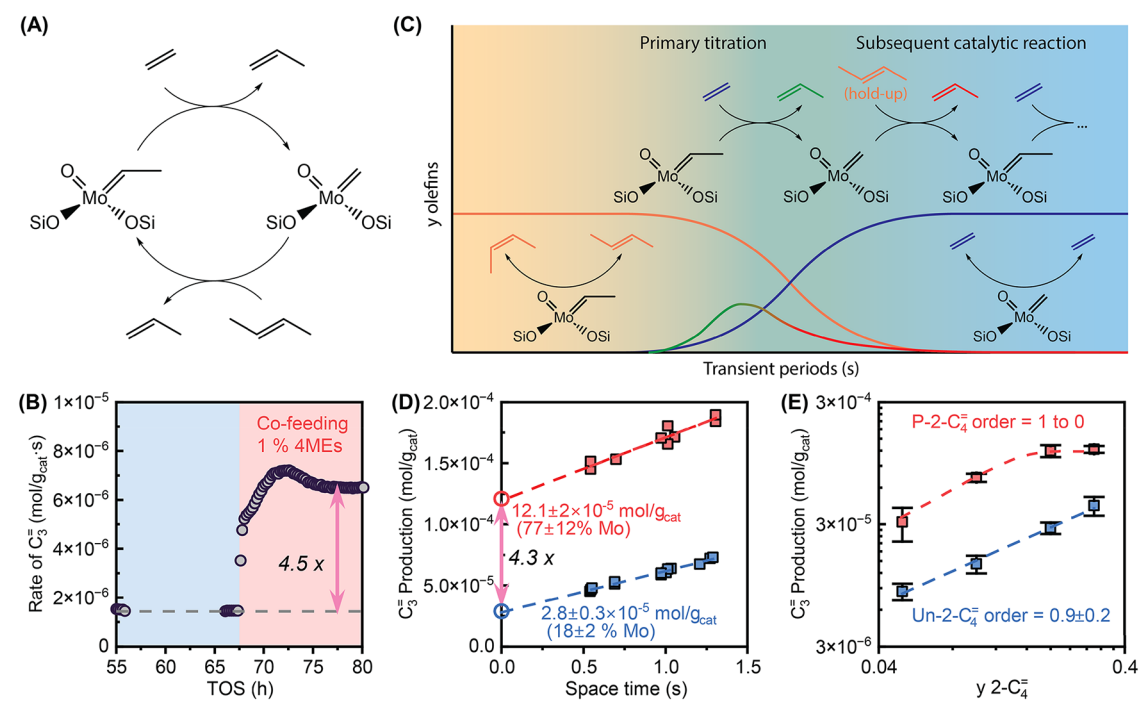


Figure 1. (A) Reaction scheme for the cross-metathesis of ethylene and 2-butenes. (B) The promotional effect in the cross-metathesis of 20% 2-butenes and 20% ethylene. Conditions: 10 mg catalyst, helium balanced, 50 mL/min total flow rate at 180 °C. (C) Reaction process for Mo ethylidene titration. (D) Propylene production during transition from 20% 2-butenes to 20% ethylene. (E) The kinetic dependence of propylene production on the partial pressure of 2-butenes. Conditions: 30 mg catalyst, helium balanced, 40 to 90 mL/min total flow rate at 180 °C. Results for unpromoted conditions are in blue color, and those for promoted conditions with 1% 4MEs cofeeding are in red color.

conventional titration methods inaccurate under steady-state conditions, as the required inert gas purging disturbs the dynamic balance of active site renewal and decay. Similar promotional effects were observed for $\text{MoO}_x/\text{SiO}_2$ catalysts, but whether their activation follows the same mechanistic pathway as WO_x/SiO_2 remained unresolved. ¹² Furthermore, the relationship between active site density and olefin concentration had not been established, making it difficult to distinguish between true increases in active site population and changes in intrinsic turnover frequency.

Here, we resolve these uncertainties by integrating precise site titration with kinetic modeling on silica-supported molybdenum oxide catalysts. To enable accurate steady-state active site titration, we employed a modified steady-state isotopic transient kinetic analysis (SSITKA) reactor adapted for nonisotopic titration. This approach circumvents the

limitations of isotopic labeling, including prohibitive cost and analytical challenges arising from m/z overlap among C_2-C_4 olefins, though it precludes direct measurement of kinetic parameters such as surface residence time and turnover frequency. Leveraging steady-state titrations under standard and promoted states, we directly quantify metathesis-active site populations under reaction conditions, revealing that up to 80% of surface Mo centers engage in the Chauvin cycle, which is a drastic increase over prior estimates that correlates directly with enhanced metathesis rates. The results demonstrate that promotion via cofed 2,3-dimethyl-2-butene isomers (4MEs) systematically increases active site density. Spectroscopic analyses using near-ambient pressure X-ray photoelectron spectroscopy (NAP-XPS) and in situ Fourier transform infrared (FTIR) spectroscopy confirm that, while 4MEs partially reduce Mo(V/VI) to Mo(IV), their primary function

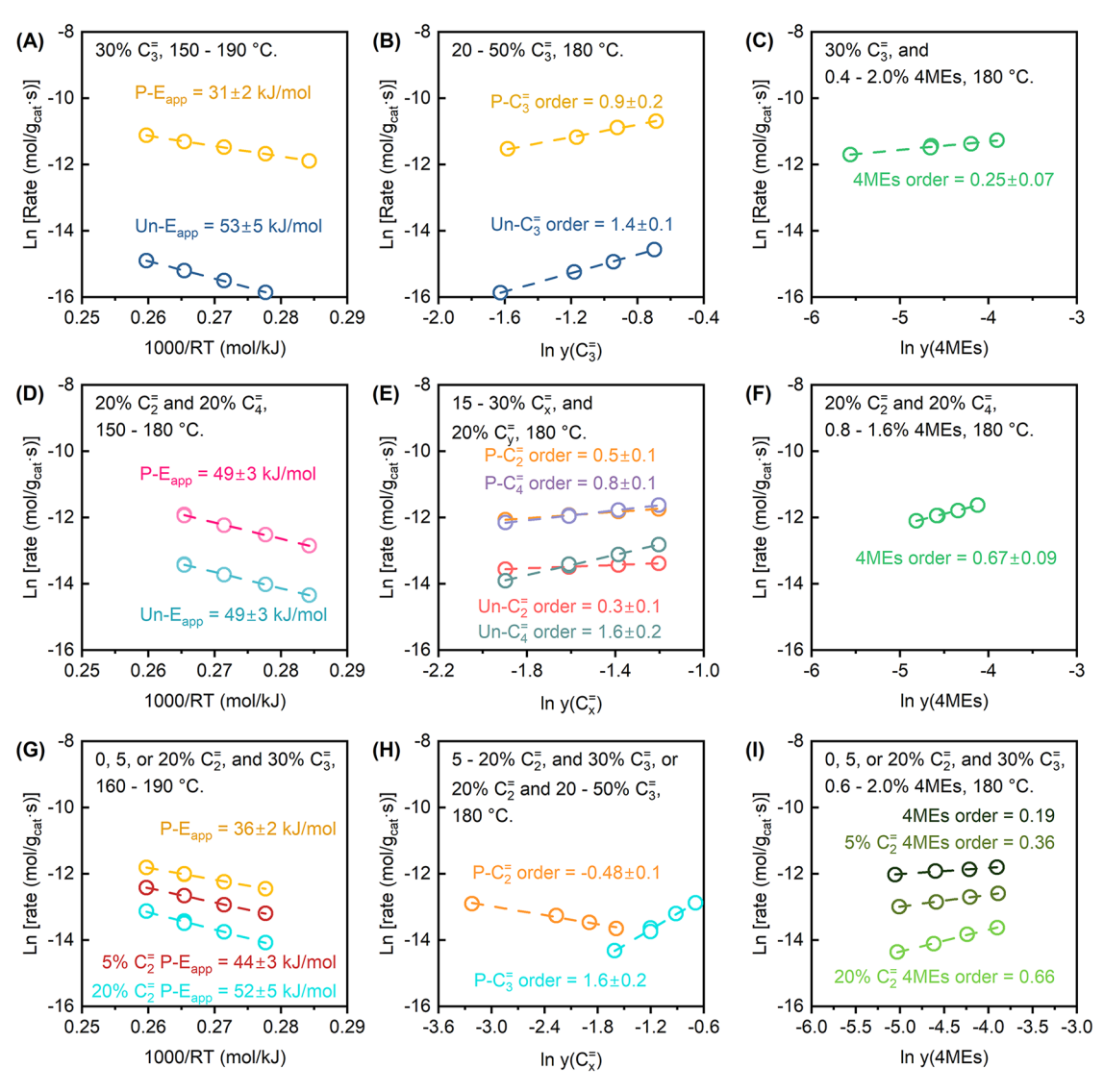


Figure 2. Kinetic parameters for olefin metathesis over 1.5% MoO_x-SOMC. (A–C) propylene $(C_3^=)$ self-metathesis, (D–F) ethylene $(C_2^=)$ and 2-butenes $(C_4^=)$ cross metathesis. (G–I) propylene $(C_3^=)$ self-metathesis with ethylene $(C_2^=)$ cofeeding, P- for promoted conditions by cofeeding 1% 4MEs and Un- for unpromoted conditions. Conditions: 15 mg catalyst, helium balanced 50 mL/min total flow.

is to facilitate proton transfer via a 1,2-proton shift mechanism that drives active site formation. Integrating these findings with kinetic modeling, we establish that 4MEs promote site renewal, saturating the surface Mo active site population and shifting the kinetic control of propylene metathesis from the site renewal and decay cycle to the Chauvin cycle. In contrast, ethylene accelerates site decay, reversing this effect and suppressing metathesis activity, providing direct evidence for its inhibitory role. Together, these insights provide a rigorous framework for linking active site density, turnover dynamics, and catalyst deactivation in heterogeneous metathesis. This work advances our understanding of site generation in Mobased metathesis catalysts and establishes selective promotion as a powerful tool for optimizing metathesis rates.

RESULTS

Promotional Effect on MoO_x-SOMC. We first investigated the promotional effect of cofeeding 4MEs in the crossmetathesis of ethylene and 2-butenes (Figure 1A) using a silica-supported molybdenum oxide catalyst with a 1.5 wt % Mo loading, synthesized via surface organometallic chemistry

 $(1.5\% \ {\rm MoO_{\it x}\text{-}SOMC}).^{15-17}$ This method yields predominantly monodispersed Mo dioxo species on silica, ¹⁵ minimizing complications from metal clusters or interface sites often present in catalysts prepared by incipient wetness impregnation. ¹⁷ Cofeeding 1% 4MEs resulted in a 4.5-fold increase in the steady-state rate of cross-metathesis (Figure 1B).

To quantify the promotional effect of 4MEs in the cross-metathesis, we performed active site titration experiments in a SSITKA type reactor with low dead volume, ensuring direct measurement of active site populations under steady-state conditions (Supporting Information Materials and Methods and Figure S1). Before titration, active sites were generated by exposing the catalyst to 20% 2-butenes for at least 12 h, a process that did not produce new olefins. Titration was initiated by switching the feed from 20% 2-butenes to 20% ethylene, leading to the exclusive formation of propylene with >99% selectivity. Propylene was produced both during the primary titration event and from subsequent catalytic reactions involving held-up 2-butenes. The linear correlation between total propylene production and space time confirmed that the reaction proceeded under differential conditions, allowing us to

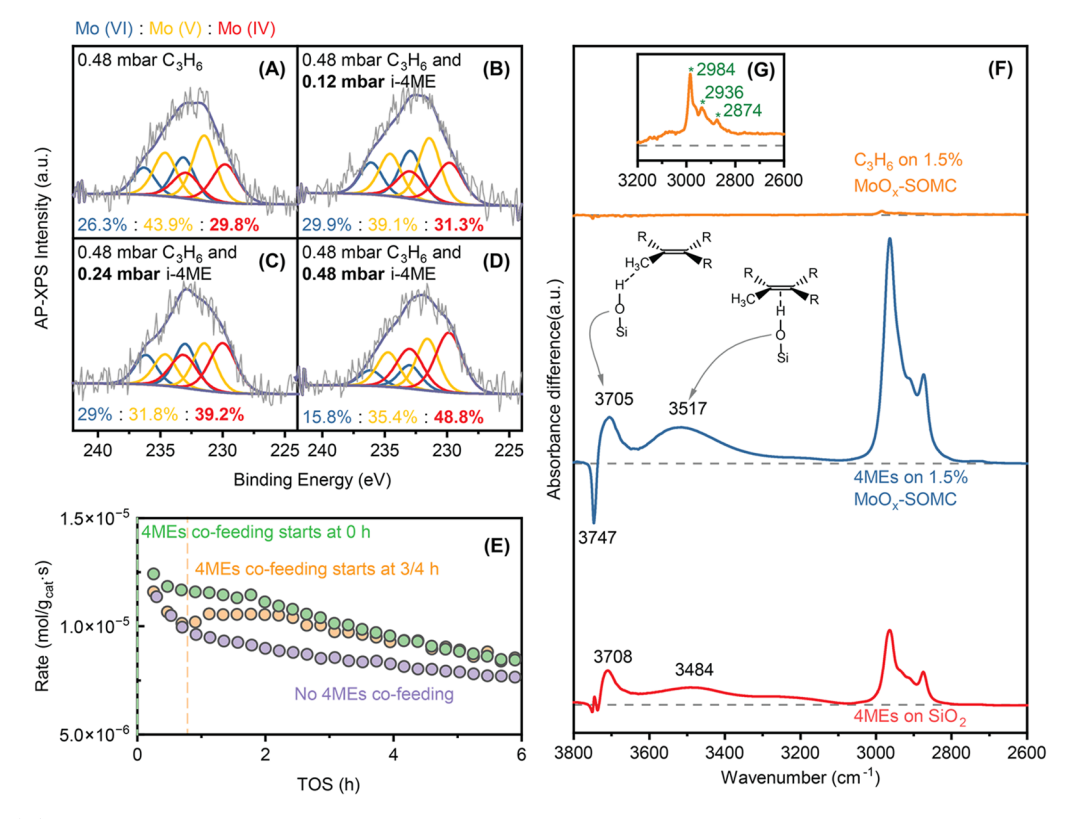


Figure 3. (A)–(D) NAP-XPS data of the Mo 3d region of the 1.5% MoO_x-SOMC catalyst subject to conditions labeled in the spectra at 250 °C. The fitted peaks for Mo(VI) are blue, Mo(V) are yellow, and Mo(IV) are red. Parameters used in peak deconvolution are listed in the Supporting Table S1. (E) The rate of propylene self-metathesis over 1.5% MoO_x-SOMC catalyst after pretreatment under 4% propylene at 550 °C. Conditions: 10-15 mg catalyst, 30% propylene in a helium balance, 50 mL/min total flow rate at 180 °C. (F) In-situ transmissive FTIR spectra of the adsorption of C_3H_6 and 4MEs on 1.5% MoO_x-SOMC, and 4MEs on SiO₂ support at 50 °C. (G) Magnified C–H stretching region of C_3H_6 on 1.5% MoO_x-SOMC. The absorbance difference was relative to the fresh catalyst after pretreatment.

extrapolate to zero space time, where catalytic conversion with 2-butenes is absent. At the y-intercept, propylene formation reflects only the primary titration event, providing a direct measure of Mo oxo ethylidene site density on the catalyst surface. For 1.5% (1.56 \times 10^{-4} mol Mo/gcat) MoO_x-SOMC, we measured 2.8 \pm 0.4 \times 10^{-5} mol/gcat of propylene from titration, corresponding to 18 \pm 3% of surface Mo sites being catalytically active (Figure 1D). Cofeeding 1% 4MEs increased active site density 4.3-fold to 12.1 \pm 0.4 \times 10^{-5} mol/gcat corresponding to 77 \pm 12% of surface Mo centers, far exceeding the previously reported maximum of \sim 20% for supported metal oxides. 4,20,21

To assess the generality of this effect, we extended the study to ${\rm MoO}_x$ and ${\rm WO}_x$ catalysts prepared by incipient wetness impregnation (IWI), a method that typically leads to more heterogeneous distributions of metal sites compared to the SOMC approach. A similar increase in active site density with 1% 4MEs cofeeding was observed across 1.4% (1.46 \times 10⁻⁴ mol Mo/g_{cat}) and 6.6% (6.88 \times 10⁻⁴ mol Mo/g_{cat}) MoO_x-IWI catalysts (3.0 \times 10⁻⁵ to 10.3 \times 10⁻⁵ mol/g_{cat} and 4.0 \times 10⁻⁵ to 12.5 \times 10⁻⁵ mol/g_{cat}, respectively), as well as 2.9% (1.58 \times 10⁻⁴ mol W/g_{cat}) WO_x-IWI catalysts (1.3 \times 10⁻⁵ to 2.5 \times 10⁻⁵ mol/g_{cat}) (Supporting Figure S3), demonstrating that the site-enhancing effect of 4MEs is not limited to MoO_x-SOMC, but extends across different catalyst formulations.

We further examined the influence of 2-butenes partial pressure on the formation of active sites. The apparent reaction order in propylene formation during titration was 0.9 with respect to 2-butenes (Figure 1E). Cofeeding 4MEs shifted the

apparent 2-butenes order from 1 to 0, revealing key mechanistic insights into active site formation.

Kinetics of Self- and Cross-Metathesis on MoO_x-SOMC. To investigate the mechanism underlying the promotional effect of 4MEs cofeeding on supported Mo catalysts, we performed kinetic studies under differential conditions, ensuring the absence of mass and heat transport limitations (Supporting Eq S3–S6). Using the 1.5% MoO_x-SOMC catalyst, we measured an apparent propylene order of 1.4 and an apparent activation energy (E_{app}) of 53 kJ/mol for propylene self-metathesis in the absence of promoter olefin (Figure 2A,B). In the cross-metathesis of 2-butenes and ethylene, we observed an ethylene order of 0.3, a 2-butenes order of 1.6, and an E_{app} of 49 kJ/mol (Figure 2D,E).

Cofeeding 1% 4MEs resulted in a 44- to 77-fold increase in the propylene self-metathesis rate under various conditions, accompanied by a reduction in the $E_{\rm app}$ from 53 to 31 kJ/mol, a decrease in the apparent propylene order from 1.4 to 0.9, and a 4MEs order of 0.25 (Figure 2A–C). In contrast, cofeeding 1% 4MEs during the cross-metathesis of ethylene and 2-butenes resulted in a more modest rate increase of 3- to 6-fold. The promoted $E_{\rm app}$ remained unchanged at 49 kJ/mol, while the promoted order for 2-butenes decreased to 0.8, the ethylene order increased to 0.5, and 4MEs exhibited an apparent order of 0.7 (Figure 2D–F).

The disparity in promotional effects observed while cofeeding 4MEs across different metathesis reactions was further investigated by introducing various olefin mixtures during propylene self-metathesis. Cofeeding 20% 2-butenes to

propylene self-metathesis increased the ethylene production rate by 4-fold. Adding 1% 4MEs to the propylene/2-butenes mixture further enhanced the rate by 7-fold relative to the propylene/2-butenes condition, and by 30-fold relative to the unpromoted propylene-only condition. In contrast, cofeeding 20% ethylene to the propylene/4MEs mixture suppressed the promoted 2-butenes formation rate by almost 80% (Supporting Figure S4). The suppression was largely reversible, with the promoted 2-butenes rate recovering to ca. 90% of its original value upon the termination of ethylene cofeeding.

To further investigate the unchanged $E_{\rm app}$ observed in crossmetathesis, we examined the poisoning effect of ethylene by introducing varying concentrations of an ethylene cofeed alongside 1% 4MEs during propylene self-metathesis. As ethylene concentration increased (Figure 2G–I), we observed a gradual rise in $E_{\rm app}$ from 36 to 52 kJ/mol, approaching the unpromoted $E_{\rm app}$ for propylene self-metathesis. Additionally, the 4MEs order increased from 0.19 to 0.66, aligning with values observed in cross-metathesis, while the propylene order unexpectedly increased to 1.6. Note that ethylene exhibited an inhibitory effect with a reaction order of -0.48, which helps explain why its net order remains lower than that of 2-butenes, even under promoted conditions.

In-Situ Spectroscopic Analysis of the Promotional **Effect.** To elucidate how 4MEs cofeeding promotes active site formation, we conducted a series of spectroscopic studies comparing the interactions of 4MEs and propylene with preactivated Mo sites. The promotional effect is expected to influence one or both of the widely proposed key factors in active site formation: (1) the reduction of Mo(VI) to lowervalent preactive Mo sites, 15,22-24 and (2) the subsequent formation of metal alkylidene species via different mechanistic pathways. 8,25,26 To examine the first factor, we investigated surface Mo reduction by i-4ME and propylene using nearambient pressure X-ray photoelectron spectroscopy (NAP-XPS). The Mo 3d region in the XPS spectra showed peaks corresponding to Mo 3d_{5/2} and Mo 3d_{3/2} for each oxidation state of Mo (Figure 3A-D). Exposure of the pretreated catalyst pellet to 0.48 mbar of propylene resulted in a surface Mo distribution of 26.3% Mo(VI), 43.9% Mo(V), and 29.8% Mo(IV) (Figure 3A). Increasing i-4ME pressure led to a monotonic increase in Mo(IV) content to 48.8%, while the fractions of Mo(VI) and Mo(V) decreased, indicating that i-4ME more effectively reduces surface Mo than propylene.

To further examine Mo reduction under reaction conditions, we used in situ diffuse reflectance (DR) UV–vis spectroscopy to monitor changes in d-d electron transitions of surface Mo cations. Cofeeding 1% 4MEs during steady-state propylene self-metathesis produced distinct absorption bands between 300 and 700 nm (Supporting Figure S8). However, the d–d transitions of Mo(VI) species overlap with π – π * transitions associated with aromatic surface species. Previous studies have reported the formation of aromatic carbon deposits on MoO_x/SiO₂ catalysts; therefore, disentangling the respective contributions of Mo d–d transitions and π -bonded carbonaceous species remains challenging. The absence of distinct C Is features in the corresponding NAP-XPS spectra suggests that carbon accumulation is minimal, and the observed spectral evolution likely reflects changes in Mo electronic structure.

Next, we investigated 4MEs cofeeding on a prereduced 1.5% MoO_x -SOMC catalyst to assess whether factors beyond Mo reduction contribute to the promotional effect. High-temperature pretreatments under olefins or alkanes have been shown

to enhance olefin metathesis rates by reducing supported metal oxides. 20,24,30 Accordingly, we preactivated the catalyst under 4% propylene at 550 °C for 30 min, minimizing further Mo reduction by 1% 4MEs at 180 °C. Despite this, introducing 1% 4MEs still enhanced catalytic activity (1.1- to 1.3-fold), albeit to a lesser extent than on a helium-activated catalyst (Figure 3E)

We used in situ transmissive Fourier transform infrared (FTIR) spectroscopy to probe surface interactions of 4MEs and propylene with the pretreated 1.5% MoO_x-SOMC catalyst. The propylene-saturated catalyst surface (Figure 3F, orange trace) exhibited a weak, broad sp³ C-H stretching region $(2800-3000 \text{ cm}^{-1})$ and a subtle decrease in the Si-OH (3747 m^{-1}) cm⁻¹) feature, with no detectable sp² C-H stretching (3000-3100 cm⁻¹). 31,32 Adsorption of 4MEs on 1.5% MoO_x-SOMC (Figure 3F, blue trace) resulted in more pronounced changes in the Si-OH (3747 cm⁻¹) feature, with significantly greater intensity reduction compared to propylene adsorption. Using an integrated molar extinction coefficient (IMEC, ε) of 1.2– 1.6,33 the estimated Si-OH consumption after 4MEs adsorption was 22 \pm 3 μ mol/g_{cat} (Supporting Figure S12). A control experiment with 4MEs adsorption on SiO₂₋₇₀₀ (dehydroxylated at 700 °C) showed minimal perturbation of isolated Si-OH (2.6 \pm 0.4 μ mol/g_{cat}), despite the presence of perturbed Si-OH groups at 3708 and 3484 cm⁻¹ (Figure 3F, red trace).

To further differentiate the interactions of 4MEs with the catalyst surface versus the SiO_2 support, temperature-programmed desorption (TPD) experiments were performed on 4MEs-saturated samples (Supporting Figure S13). On SiO_{2-700} , all surface species fully desorbed by 120 °C. In contrast, on the MoO_x -SOMC catalyst, desorption occurred continuously over a broader temperature range, extending to significantly higher temperatures than on the support. Although most surface-bound 4MEs desorbed by 180 °C, residual IR signals in the C–H stretching region persisted.

DISCUSSION

In heterogeneous olefin metathesis, olefins fulfill multiple mechanistic roles. They generate active metal alkylidene species from preactive sites, undergo metathesis with these species, and, in specific cases such as ethylene, promote deactivation.^{34,35} Thus, the population of active sites is dynamic, continuously renewed and lost under reaction conditions, which complicates direct quantification. To approximate the steady-state active site density during crossmetathesis of 2-butenes and ethylene, MoO_x-SOMC was first exposed to 20% 2-butenes. Although no metathesis products were detected under flowing 2-butenes, switching the feed to 20% ethylene led to the immediate and selective formation of propylene. This observation confirms that 2-butenes form Mo ethylidene species, which do not react productively with 2-butenes but readily undergo metathesis with ethylene to produce propylene.

Steady-state titration experiments showed that cofeeding 1% 4MEs increases the Mo ethylidene density by 4.3-fold. This increase closely matches the 4.5-fold enhancement in the steady-state rate of cross-metathesis between 2-butenes and ethylene, indicating that the promotional effect of 4MEs primarily arises from an increase in active site density.

The apparent 2-butenes order of 0.9 for Mo ethylidene formation indicates that site generation is kinetically relevant under unpromoted conditions and helps rationalize previously

reported olefin orders exceeding the 0-1 range predicted by the Chauvin cycle. With 1% 4MEs cofeeding, the first-order dependence on 2-butenes at low concentrations demonstrates that 4MEs accelerate site formation but do not independently create active sites. At higher 2-butenes concentrations (>20%), the order decreases to zero, indicating saturation of Mo oxo ethylidene coverage, with up to \sim 80% of surface Mo engaged in turnover.

Having established the kinetic relevance and saturation behavior of site formation, we next evaluated the kinetics of the metathesis reactions under different feed conditions. In the absence of promoter olefins, the apparent reaction orders of propylene (1.4) and 2-butenes (1.6) exceed the 0-1 range predicted by the Chauvin cycle, consistent with their participation in additional kinetically relevant steps. In contrast, ethylene exhibits a much lower order (0.3), consistent with a limited role in site formation. Given that 2-butenes exhibit a reaction order of 0.9 in Mo ethylidene formation, the elevated apparent orders of propylene and 2-butenes likely reflect their dual roles in kinetically relevant active site formation and metathesis. The low reaction order for ethylene likely reflects its competing role as a site-poisoning species, which limits its participation in site renewal or related pathways.

Cofeeding 1% 4MEs lowers the reaction orders of propylene and 2-butenes to values consistent with Chauvin cycle predictions, while 4MEs themselves exhibit nonzero orders despite not undergoing metathesis. This indicates that 4MEs participate in kinetically relevant steps involved in active site formation, substituting for the reactant olefins in these processes. Notably, the 4MEs reaction orders differ between the metathesis reactions. Analysis of apparent 4MEs orders provides insights into whether overall reaction kinetics are governed by the site renewal and decay cycle or the Chauvin cycle. On 1.5% MoO_r -SOMC, the lower 4MEs order of 0.2 in propylene self-metathesis implies a less kinetically relevant site renewal and decay cycle. In previous studies, Grünert et al. reported that the propylene reaction order ranged from 0.78 to 0.84 on MoO_x/Al₂O₃ catalysts, with apparent activation energies between 30 and 38 kJ/mol.³⁶ These values, which align with the promoted MoO_x-SOMC case (31 kJ/mol), reflect kinetic control of the Chauvin cycle with minimal contribution from active site formation. Conversely, in our previous kinetic study on 3% WO_x-SOMC, $E_{\rm app}$ decreased from 156 to 116 kJ/mol with a 4MEs order of 0.8. The nearunity 4MEs order suggests that the site renewal and decay cycle was kinetically relevant, and the observed decrease in $E_{\rm app}$ likely reflects differing activation barriers for propylene and 4MEs in this cycle.

In promoted cross-metathesis, the 4MEs order of 0.7 suggests that active site formation remains kinetically relevant. Using SSITKA-derived turnover frequencies to decouple metathesis turnover from site renewal and decay, Zhang et al. reported an apparent activation energy of 35 kJ/mol for the same reaction over a similar MoO_x/SiO_2 catalyst, representing the intrinsic kinetics of the Chauvin cycle.³⁷ The E_{app} in our system remains at 49 kJ/mol, indicating that the overall reaction remains under kinetic control by the site renewal and decay cycle. Moreover, the unchanged E_{app} upon 4MEs cofeeding suggests that the activation barriers associated with 4MEs- and 2-butenes-assisted site formation are comparable.

Additional evidence arises from promoted propylene selfmetathesis in the presence of cofed ethylene. Introducing 20% ethylene increases the 4MEs reaction order from 0.2 to 0.7 and raises the promoted $E_{\rm app}$ from 36 to 52 kJ/mol, a value comparable to the unpromoted $E_{\rm app}$ for propylene self-metathesis. These changes indicate that ethylene reduces the steady-state population of Chauvin intermediates through a competitive adsorption or site-blocking mechanism and shifts the kinetic regime from metathesis turnover to site renewal and decay. The similarity in $E_{\rm app}$ across different olefins further suggests that, unlike in 3% WO_x-SOMC, the barriers associated with site dynamics involving propylene, 2-butenes, and 4MEs are comparable on 1.5% MoO_x-SOMC.

Kinetic analysis provides a clear basis for understanding why cofeeding 1% 4MEs leads to a much larger rate enhancement in propylene self-metathesis than in cross-metathesis. Given that the promotional effects of 4MEs cofeeding originate from increases in active site populations, differences in promotional magnitude across reactions likely reflect variations in the extent of site population increase. In the absence of promoter olefins, kinetic data indicate that both propylene and 2-butenes contribute to active site formation in their respective reactions. The 4-fold increase in ethylene production rate while cofeeding 20% 2-butenes to propylene self-metathesis indicates that 2-butenes are more effective than propylene in facilitating active site formation. Adding 1% 4MEs to the propylene/2butenes mixture further boosts the rate by 7-fold, and by 30fold compared to the propylene-only condition. These results suggest that 2-butenes already drive a higher degree of site formation than propylene, limiting the additional enhancement achievable by 4MEs. In addition, the higher ethylene concentration required in cross-metathesis, compared to that generated in self-metathesis, exacerbates site deactivation and could partly account for the smaller promotional effect of 4MEs under these conditions.

Spectroscopic results provide complementary evidence for the role of 4MEs in promoting metathesis. NAP-XPS confirms that i-4ME reduces surface Mo(VI) species more readily than propylene. However, a measurable promotional effect persists even on prereduced catalysts, indicating that Mo reduction alone does not account for the observed rate enhancement. The promoted rate deactivates to the unpromoted level under standard conditions once 4MEs are removed, suggesting that their effect depends on continuous cofeeding. Together, these findings point to an additional mechanistic role for 4MEs beyond Mo reduction.

In situ FTIR shows that 4MEs interact more strongly with surface silanol groups than propylene does, particularly with those perturbed by adjacent Mo centers. Upon 4MEs exposure, the intensity of these Mo-perturbed Si-OH signals decreases significantly on the catalyst, whereas similar features remain largely unchanged on the SiO₂ support. Prior studies have shown that metal-perturbed silanols exhibit stronger Brønsted acidity due to electronic interactions with neighboring high-valent metal centers. ^{13,14,38,39} The selective depletion of the Mo-perturbed Si-OH upon 4MEs adsorption reflects its enhanced acidity, which was also supported by CD3CN adsorption experiments (Supporting Figure S7) and prior solid-state NMR studies. 12 This acidity enables protonation of electron-rich olefins like 4MEs, facilitating the formation of surface-bound carbocations or alkoxides. Such species have been identified in WO_x-SOMC systems by IR and NMR;¹² similar intermediates likely form on Mo-based catalysts as well. The greater extent of 4MEs adsorption relative to propylene likely results from both their lower volatility and the stabilizing

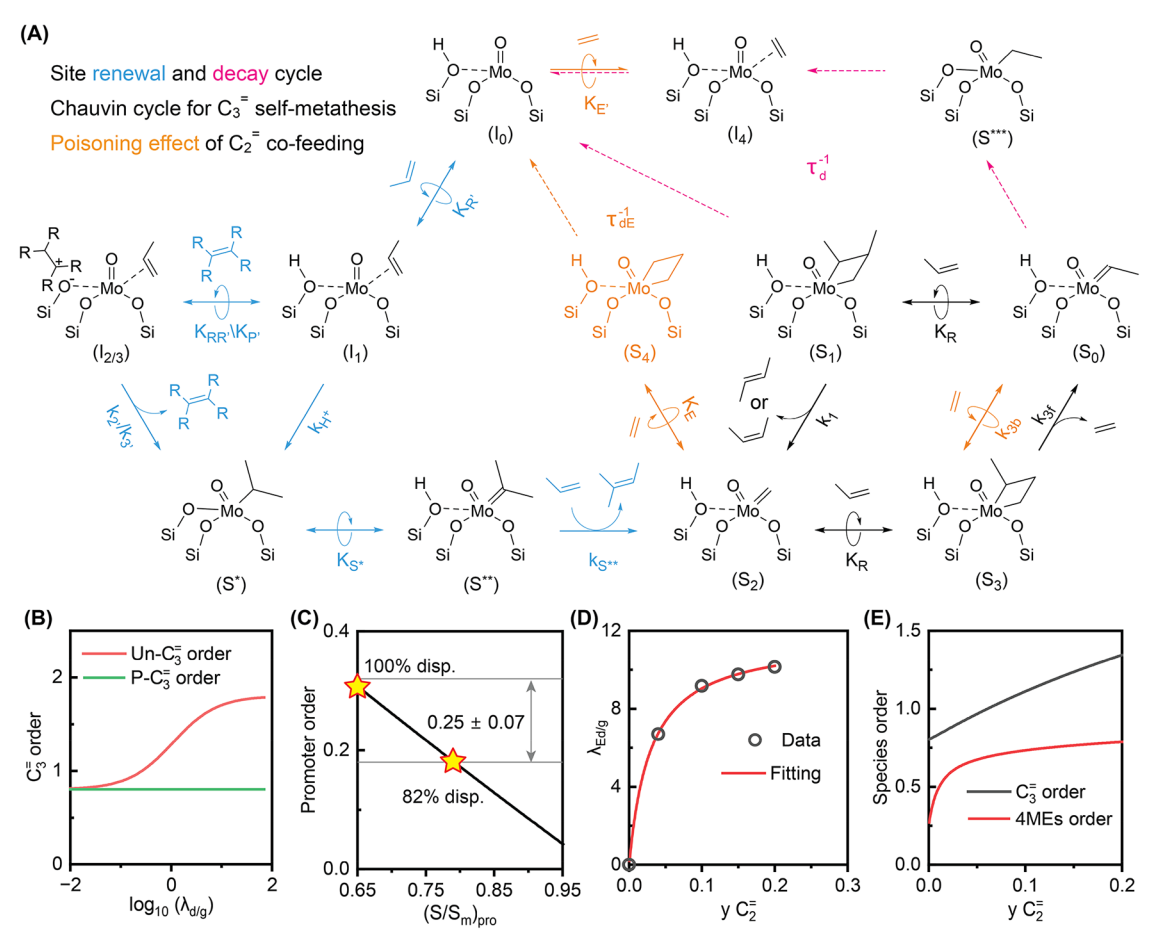


Figure 4. (A) Proposed reaction mechanism for propylene self-metathesis over MoO_x/SiO_2 . Subscript R and 2 (e.g., K_R , $K_{RR'}$, k_2 , or I_2) stand for propylene, P and 3 for 4MEs, E for ethylene; τ_d^{-1} for site decay rate, and τ_{dl}^{-1} for ethylene-assisted site decay rate. (B) The influence of the ratio ($\lambda_{d/g}$) of decay rate to propylene-assisted site renewal rate on propylene orders. (C) The estimated fractions of monodispersed surface $Mo(S_m)$ and Chauvin cycle intermediates (S) on 1.5% MoO_x -SOMC. (D) Sum-of-squares error fitting of experimental data to the Michaelis—Menten equation to determine the ratio of ethylene-assisted site decay rate to propylene-assisted site renewal rate ($\lambda_{Ed/g}$). (E) The simulated effect of ethylene cofeeding on promoted propylene and 4MEs orders.

effect of methyl substituents, which facilitate positive charge formation.

Proton transfer has been frequently implicated as the ratelimiting step in the conversion of Mo dioxo precursors into catalytically active alkylidene species. 40,41 Recent studies on homogeneous Mo and W organometallic complexes suggest that proton transfer from proton donors to styrene-bound Mo and W species is the rate-determining step for alkylidene formation. Computational studies further indicate that proton transfer barriers, from Mo perturbed Si-OH to propylene adsorbed on Mo(IV) and from Mo isopropyl complexes to Mo-O-Si bridge oxygens, represent the highest energy barriers in Mo oxo propylidene formation. 44 Based on these insights, we propose that 4MEs promote the formation of surface-bound carbocations or alkoxides that, upon desorption, release labile protons. These protons then drive the 1,2-proton shift step that enables active site formation, thereby accelerating alkylidene generation and sustaining high metathesis rates under promoted conditions.

Building upon our kinetic and spectroscopic insights, we propose a mechanistic framework (Figure 4A) that integrates the Chauvin cycle with site renewal and decay processes, providing a unified explanation for the observed kinetic behavior exceeding Chauvin cycle predictions. The mechanism begins with partially reduced Mo(IV) (I_0), generated through

helium pretreatment at 500 °C, as confirmed by NAP-XPS measurements and previous studies identifying it as the preactive site. 14,17,30 Under steady-state reaction conditions, site renewal (blue pathway) occurs via a 1,2-proton shift mechanism mediated by proximal silanol groups, generating Mo oxo alkylidene sites with a reaction order between 0 and 1 for propylene or 4MEs. Alongside site decay pathways (red dashed line), 42,43 which remain insensitive to propylene partial pressure (Supporting Figure S7A), this renewal-decay cycle dynamically regulates the population of Chauvin cycle intermediates, thereby modulating the steady-state metathesis rate. Leveraging previous experimental and theoretical along with the observed propylene reaction order range (0-2), we propose the proton transfer step generating the Mo oxo isopropyl intermediate (S^*) serves as the rate-limiting step for site renewal. In this framework, 4MEs could enhance active site formation by either increasing the surface coverage of intermediate $(I_{2/3})$ leading to S^* or lowering the barrier for the proton transfer $(k_{2'}/k_{3'})$ forming S*. In addition, the adsorption of 4MEs on Lewis acidic Mo sites could also lead to the formation of a surface Mo-alkyl adduct, which may undergo β -H elimination to generate 4MEs and a Mo-H species frequently proposed in the literature as a plausible intermediate in metathesis active site formation. Such Mo-H species could further promote propylene insertion to

yield a Mo alkylidene. 14,38,45 However, no corresponding Mo— H features, typically observed between 1600 and 2000 cm⁻¹,46,47 were detected in the FTIR spectra after 4MEs adsorption, though this possibility warrants further investigation.

To evaluate the consistency between the proposed mechanism and experimental trends, we developed a kinetic model containing two interdependent cycles: an active site renewal and decay cycle and the Chauvin cycle (Supporting Information Material and Methods and Section 16). Both cycles share the same surface network involving metathesisinactive species (I_i) and active sites (S_i) . By solving the renewal and decay cycle, we obtained an analytical expression for the steady-state active site fraction, $S/S_{\rm m}$, where S represents the concentration of active sites and $S_{\rm m}$ denotes the total number of surface sites. The rate expression for 2-butenes formation is then obtained from the Chauvin cycle but weighted by S/S_{m} , thereby coupling metathesis turnover with the dynamics of site renewal and decay. All rate expressions were derived analytically from elementary steps using quasi-equilibrium and quasi-steady-state approximations, yielding a closed-form framework that links feed composition, site dynamics, and observed metathesis rates.

The assumption that all I_i sites are chemically identical could not reproduce the 0.5 decrease in propylene order upon promotion, indicating that preactive sites are chemically heterogeneous (Supporting Section 18). Given the renewal pathway proceeds through a 1,2-proton shift, differences in silanol acidity are expected to influence site activation. This motivated us to propose a two-site hypothesis wherein β -sites, which are sufficiently acidic to be activated by both propylene and 4MEs, coexist with α -sites with weaker acidity, which require exclusively 4MEs for activation (Supporting Information Material and Methods). Fitting the model to the change in propylene order upon promotion revealed that β -sites constitute only 3% of $S_{\rm m}$, while α -sites account for 97%. This distribution is consistent with IR data (Figure 3F), which showed much stronger interactions of 4MEs with silanols than those of propylene.

Parameter estimation using experimental data (Supporting Section 18) revealed that propylene orders (Figure 4B) are governed by two key factors: the propylene adsorption constant (KR) and the ratio of site decay rate to the propylene-assisted site renewal rate ($\lambda_{d/g}$). While K_R influences both promoted and unpromoted conditions through its role in the Chauvin cycle, $\lambda_{\rm d/g}$ determines the steady-state balance of site renewal and decay, and thus primarily affects the unpromoted order. The optimal $K_{\rm R}$ value was estimated from the promoted order (Supporting Figure S17), and $\lambda_{d/g}$ was screened to match the unpromoted order. At high values of $\lambda_{\rm d/g}$, where decay dominates over renewal, $S/S_{\rm m}$ is low, and the difference in propylene orders upon promotion approached unity. As $\lambda_{\rm d/g}$ decreases, renewal dominates, $S/S_{\rm m}$ increases, and the difference in orders diminishes, reflecting a transition toward Chauvin control. This trend is consistent with catalysts with higher Brønsted acidity, which enhance the protonassisted renewal pathway (k_{H+} , Figure 4A), thereby decreasing $\lambda_{d/g}$. At the same temperature as the order measurements, steady-state titrations show S/S_m of only 8.2% on WO_x-IWI compared to 20.6% on MoO_x -IWI, despite similar S_m values (2.9 vs 1.4 wt %), implying that the difference arises from a higher $\lambda_{d/g}$ on W. With similar promoted propylene orders of 0.9, the higher unpromoted propylene order on WO_x (1.9)

relative to MoO_x (1.4) supports the model prediction that higher $\lambda_{\text{d/g}}$ values produce larger order differences upon promotion.

For the 1.5% MoO_x-SOMC catalyst, the experimentally observed unpromoted propylene order of 1.4 corresponds to a moderate $\lambda_{d/g}$ value of 1.6. Alternatively, $\lambda_{d/g}$ may be altered by increasing the rate of generation. In cross-metathesis, the reduced promotional effect may be due to the natural promotion ability of 2-butenes, which lead to a higher $k_{\rm gR} R$ and therefore a lower $\lambda_{d/g}$. This framework also clarifies why 4MEs appear less effective in cross-metathesis than in selfmetathesis. In cross-metathesis, 2-butenes already provide a faster renewal pathway ($k_{\rm gR}$ R), which lowers $\lambda_{\rm d/g}$ and reduces the relative impact of 4MEs compared to propylene. At the same time, ethylene accelerates decay, further limiting the promotional effect. The higher unpromoted 2-butenes order, despite lower $\lambda_{d/g}$ can be attributed to this ethylene-assisted decay pathway, which elevates the apparent olefin order and partially obscures the role of renewal.

The 4MEs order primarily depends on surface site dispersion and the titration value of promoted active sites $(77 \pm 12\%)$. Analysis of the promoter reaction order relative to site occupancy $(S/S_{\rm m})$ (Figure 4C) indicates a site occupancy of 0.72 ± 0.07 for the observed 4MEs reaction order of 0.25 ± 0.07 , implying a dispersion fraction of 83-100% for the 1.5% MoO_x-SOMC catalyst. A similar order-matching analysis for the 6.6% MoO_x-IWI catalyst showed reasonable consistency in the atomic dispersion fraction within the error range of the promoter reaction order (Supporting Figure S16). These results validate that the model quantitatively captures the link between 4MEs kinetics and site availability across distinct catalyst architectures.

Analysis of catalyst deactivation during ethylene cofeeding was used to assess whether the observed increases in propylene and promoter reaction orders could be fully explained by surface coverage effects on I_i and S_i sites (Supporting Section 19). The ethylene-assisted decay ratio $(\lambda_{\rm Ed/g})$ was modeled using a Michaelis-Menten-type expression (Figure 4D), revealing that ethylene induces kinetic decay steps following a pre-equilibrium stage. These results point to a dual role for ethylene as (1) enhancing the saturation of a reactive intermediate and (2) facilitating secondary decay pathways. During propylene self-metathesis under differential conditions, the limited formation of ethylene restricts intermediate accumulation and minimizes decay. By contrast, ethylene cofeeding accelerates these deactivation processes, leading to higher propylene and 4MEs reaction orders. Simulated reaction orders in the presence of 20% ethylene cofeed were 1.35 for propylene and 0.78 for 4MEs, consistent with the experimentally determined ethylene reaction order of -0.5 (Supporting Figure S22).

Taken together, the kinetic model provides quantitative validation of the proposed mechanism across a range of reaction conditions. It captures the distinct propylene reaction orders observed under promoted and unpromoted regimes through a two-site framework grounded in variations in silanol acidity. The model demonstrates that the relative rates of site renewal and decay, reflected by the parameter $\lambda_{\rm d/g}$ determine which steps control the overall reaction rate across different catalysts. It also links the promoter reaction order to the degree of surface site occupancy, in agreement with independent titration-based estimates of metal dispersion. Furthermore, the model accounts for the increase in reaction orders under

ethylene cofeeding through a kinetic decay pathway modeled by a pre-equilibrium-limited Michaelis—Menten expression. Within this framework, the stronger promotional effect observed in self-metathesis arises from the relatively high $\lambda_{\rm d/g}$ associated with propylene-assisted renewal, whereas in cross-metathesis, faster renewal by 2-butenes and simultaneous ethylene-assisted decay yield lower effective $\lambda_{\rm d/g}$ values and a smaller relative impact of 4MEs. Collectively, these results support a unified mechanistic picture in which metathesis kinetics are governed not only by the intrinsic steps of the Chauvin cycle but also by the dynamic balance between site formation and decay.

Finally, comparative studies with MoO_x-IWI catalysts (Supporting Section 20), which contain monomolybdates, polymolybdates, and MoO₃ crystalline clusters, show an inverse correlation between promotional effect and Mo loading, except for the 14.2% MoO_x-IWI catalyst, suggesting that dispersed molybdate species near Si-OH groups benefit most from promotion. These findings offer a framework for optimizing metathesis catalysts through site engineering, with ongoing efforts focused on refining the interplay between Mo dispersion, reducibility, and Brønsted acidity to further control site accessibility and stability. Future work will integrate renewal and decay kinetics across a broader range of catalysts to develop a predictive approach for tuning metathesis activity and mitigating deactivation pathways.

CONCLUSION

This study develops a mechanistic framework for active site generation, renewal, and decay to elucidate the kinetic behavior of silica-supported molybdenum oxide catalysts in heterogeneous olefin metathesis. By combining steady-state titration, in situ spectroscopy, and kinetic modeling, we show that substituted olefins (4MEs) promote a 1,2-proton shift mechanism that accelerates Mo oxo alkylidene formation and increases active site density by up to 4.3-fold. This promotional effect significantly boosts the steady-state rate of propylene self-metathesis, shifting kinetic control from the active site renewal and decay cycle to the Chauvin cycle. In contrast, ethylene acts as a decay promoter, accelerating active site deactivation and returning kinetic control to the site renewal and decay cycle. In addition, studies on MoOx-IWI catalysts further demonstrate that the promotional effect is strongest for dispersed molybdate species and diminishes with increasing Mo loading and MoO₃ crystallinity. Together, these results establish a quantitative link between active site population and metathesis kinetics, providing a predictive basis for catalyst design. By elucidating the interplay between site renewal, decay, and catalytic turnover, this study offers new strategies to enhance active site accessibility and mitigate deactivation pathways.

ASSOCIATED CONTENT

Supporting Information

The Supporting Information is available free of charge at https://pubs.acs.org/doi/10.1021/jacs.5c15418.

Experimental details, additional catalytic reactivity data, additional catalyst characterization, estimation of transport criteria, and details of the kinetic model formulation (PDF)

AUTHOR INFORMATION

Corresponding Author

Yuriy Román-Leshkov — Department of Chemical Engineering, Massachusetts Institute of Technology, Cambridge, Massachusetts 02139, United States; orcid.org/0000-0002-0025-4233; Email: yroman@mit.edu

Authors

Ran Zhu – Department of Chemical Engineering, Massachusetts Institute of Technology, Cambridge, Massachusetts 02139, United States

Griffin Drake — Department of Chemical Engineering, Massachusetts Institute of Technology, Cambridge, Massachusetts 02139, United States

Husain H. Adamji — Department of Chemical Engineering, Massachusetts Institute of Technology, Cambridge, Massachusetts 02139, United States; ● orcid.org/0000-0003-3058-680X

Zachariah J. Berkson — Department of Chemistry and Applied Bioscience, ETH Zürich, CH-8093 Zürich, Switzerland; School for Engineering of Matter, Transport and Energy, Arizona State University, Tempe, Arizona 85287, United States; Occid.org/0000-0002-2157-4172

Jie Zhu – Department of Chemical Engineering, Massachusetts Institute of Technology, Cambridge, Massachusetts 02139, United States

Ashley R. Head — Center for Functional Nanomaterials, Brookhaven National Laboratory, Upton, New York 11973, United States; Occid.org/0000-0001-8733-0165

Heather J. Kulik – Department of Chemical Engineering, Massachusetts Institute of Technology, Cambridge, Massachusetts 02139, United States; ⊚ orcid.org/0000-0001-9342-0191

Christophe Copéret – Department of Chemistry and Applied Bioscience, ETH Zürich, CH-8093 Zürich, Switzerland

Complete contact information is available at: https://pubs.acs.org/10.1021/jacs.5c15418

Notes

The authors declare no competing financial interest.

ACKNOWLEDGMENTS

The MIT authors acknowledge the U.S. Department of Energy, Office of Basic Energy Sciences under Award DE-SC0016214 for the financial support as well as the National Science Foundation under CBET-1846426. This research used the Proximal Probes Facility of the Center for Functional Nanomaterials (CFN), which is a U.S. Department of Energy Office of Science User Facility, at Brookhaven National Laboratory under Contract No. DE-SC0012704. The authors acknowledge Bowei Liu and Xianyuan Wu for their feedback on the manuscript.

REFERENCES

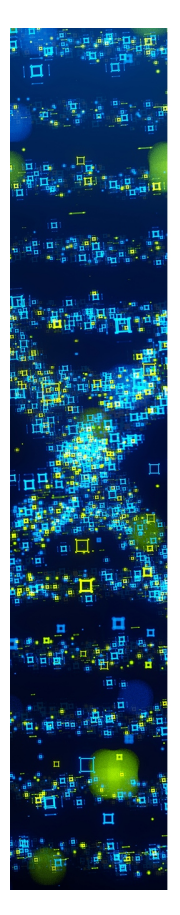
ī

- (1) Keim, W. Oligomerization of Ethylene to α -Olefins: Discovery and Development of the Shell Higher Olefin Process (SHOP). *Angew. Chem., Int. Ed.* **2013**, 52 (48), 12492–12496.
- (2) Mol, J. Industrial applications of olefin metathesis. J. Mol. Catal. A: Chem. 2004, 213 (1), 39–45.
- (3) Chauvin, Y. Olefin metathesis: The early days (Nobel lecture). Angew. Chem., Int. Ed. 2006, 45 (23), 3740–3747.

- (4) Lwin, S.; Wachs, I. E. Olefin Metathesis by Supported Metal Oxide Catalysts. ACS Catal. 2014, 4 (8), 2505-2520.
- (5) Casey, C. P.; Burkhardt, T. J. Reactions of (diphenylcarbene) pentacarbonyltungsten (0) with alkenes. Role of metal-carbene complexes in cyclopropanation and olefin metathesis reactions. *J. Am. Chem. Soc.* 1974, 96 (25), 7808–7809.
- (6) Jean-Louis Hérisson, P.; Chauvin, Y. Catalyse de transformation des oléfines par les complexes du tungstène. II. Télomérisation des oléfines cycliques en présence d'oléfines acycliques. *Macromol. Chem. Phys.* **1971**, *141* (1), *161–176*.
- (7) Hoveyda, A. H.; Zhugralin, A. R. The remarkable metal-catalysed olefin metathesis reaction. *Nature* **2007**, *450* (7167), No. 243.
- (8) Howell, J. G.; Li, Y.-P.; Bell, A. T. Propene metathesis over supported tungsten oxide catalysts: A study of active site formation. *ACS Catal.* **2016**, *6* (11), 7728–7738.
- (9) Mougel, V.; Chan, K.-W.; Siddiqi, G.; Kawakita, K.; Nagae, H.; Tsurugi, H.; Mashima, K.; Safonova, O.; Copéret, C. Low Temperature Activation of Supported Metathesis Catalysts by Organosilicon Reducing Agents. ACS Cent. Sci. 2016, 2 (8), 569–576.
- (10) Conk, R. J.; Stahler, J. F.; Shi, J. X.; Yang, J.; Lefton, N. G.; Brunn, J. N.; Bell, A. T.; Hartwig, J. F. Polyolefin waste to light olefins with ethylene and base-metal heterogeneous catalysts. *Science* **2024**, 385 (6715), 1322–1327.
- (11) Conk, R. J.; Hanna, S.; Shi, J. X.; Yang, J.; Ciccia, N. R.; Qi, L.; Bloomer, B. J.; Heuvel, S.; Wills, T.; Su, J.; et al. Catalytic deconstruction of waste polyethylene with ethylene to form propylene. *Science* **2022**, *377* (6614), 1561–1566.
- (12) Gani, T. Z. H.; Berkson, Z. J.; Zhu, R.; Kang, J. H.; Di Iorio, J. R.; Chan, K. W.; Consoli, D. F.; Shaikh, S. K.; Copéret, C.; Román-Leshkov, Y. Promoting active site renewal in heterogeneous olefin metathesis catalysts. *Nature* **2023**, *617* (7961), 524–528.
- (13) Liu, S.; Boudjelel, M.; Schrock, R. R.; Conley, M. P.; Tsay, C. Interconversion of Molybdenum or Tungsten d2 Styrene Complexes with d0 1-Phenethylidene Analogues. *J. Am. Chem. Soc.* **2021**, *143* (41), 17209–17218.
- (14) Amakawa, K.; Wrabetz, S.; Kröhnert, J.; Tzolova-Müller, G.; Schlögl, R.; Trunschke, A. In situ generation of active sites in olefin metathesis. *J. Am. Chem. Soc.* **2012**, *134* (28), 11462–11473.
- (15) Berkson, Z. J.; Zhu, R.; Ehinger, C.; Latsch, L.; Schmid, S. P.; Nater, D.; Pollitt, S.; Safonova, O. V.; Bjorgvinsdottir, S.; Barnes, A. B.; Roman-Leshkov, Y.; Price, G. A.; Sunley, G. J.; Coperet, C. Active Site Descriptors from (95)Mo NMR Signatures of Silica-Supported Mo-Based Olefin Metathesis Catalysts. J. Am. Chem. Soc. 2023, 145 (23), 12651–12662.
- (16) Berkson, Z. J.; Bernhardt, M.; Schlapansky, S. L.; Benedikter, M. J.; Buchmeiser, M. R.; Price, G. A.; Sunley, G. J.; Copéret, C. Olefin-surface interactions: a key activity parameter in silicasupported olefin metathesis catalysts. *JACS Au* 2022, 2 (3), 777–786.
- (17) Yamamoto, K.; Chan, K. W.; Mougel, V.; Nagae, H.; Tsurugi, H.; Safonova, O. V.; Mashima, K.; Copéret, C. Silica-supported isolated molybdenum di-oxo species: formation and activation with organosilicon agent for olefin metathesis. *Chem. Commun.* **2018**, *54* (32), 3989–3992.
- (18) Ledesma, C.; Yang, J.; Chen, D.; Holmen, A. Recent approaches in mechanistic and kinetic studies of catalytic reactions using SSITKA technique. ACS Catal. 2014, 4 (12), 4527–4547.
- (19) Shannon, S. L.; Goodwin, J. G., Jr Characterization of catalytic surfaces by isotopic-transient kinetics during steady-state reaction. *Chem. Rev.* **1995**, 95 (3), 677–695.
- (20) Ding, K.; Gulec, A.; Johnson, A. M.; Drake, T. L.; Wu, W.; Lin, Y.; Weitz, E.; Marks, L. D.; Stair, P. C. Highly efficient activation, regeneration, and active site identification of oxide-based olefin metathesis catalysts. *ACS Catal.* **2016**, *6* (9), 5740–5746.
- (21) Zhang, B.; Xiang, S.; Frenkel, A. I.; Wachs, I. E. Molecular Design of Supported MoO x Catalysts with Surface TaO x Promotion for Olefin Metathesis. *ACS Catal.* **2022**, *12* (5), 3226–3237.
- (22) Amakawa, K.; Sun, L.; Guo, C.; Hävecker, M.; Kube, P.; Wachs, I. E.; Lwin, S.; Frenkel, A. I.; Patlolla, A.; Hermann, K.; et al. How

- strain affects the reactivity of surface metal oxide catalysts. Angew. Chem., Int. Ed. 2013, 52 (51), 13553-13557.
- (23) Wu, J. F.; Ramanathan, A.; Kersting, R.; Jystad, A.; Zhu, H.; Hu, Y.; Marshall, C. P.; Caricato, M.; Subramaniam, B. Enhanced Olefin Metathesis Performance of Tungsten and Niobium Incorporated Bimetallic Silicates: Evidence of Synergistic Effects. *Chem-CatChem* **2020**, *12* (7), 2004–2013.
- (24) Myradova, M.; Węgrzynowicz, A.; Węgrzyniak, A.; Gierada, M.; Jodłowski, P.; Łojewska, J.; Handzlik, J.; Michorczyk, P. Tuning the metathesis performance of a molybdenum oxide-based catalyst by silica support acidity modulation and high temperature pretreatment. *Catal. Sci. Technol.* **2022**, *12* (7), 2134–2145.
- (25) Kondratenko, V. A.; Hahn, T.; Bentrup, U.; Linke, D.; Kondratenko, E. V. Metathesis of ethylene and 2-butene over MoOx/Al2O3-SiO2: Effect of MoOx structure on formation of active sites and propene selectivity. *J. Catal.* **2018**, *360*, 135–144.
- (26) Amakawa, K.; Kröhnert, J.; Wrabetz, S.; Frank, B.; Hemmann, F.; Jäger, C.; Schlögl, R.; Trunschke, A. Active sites in olefin metathesis over supported molybdena catalysts. *ChemCatChem* **2015**, 7 (24), 4059–4065.
- (27) Chakrabarti, A.; Wachs, I. E. Molecular Structure–Reactivity Relationships for Olefin Metathesis by Al2O3-Supported Surface MoO x Sites. *ACS Catal.* **2018**, 8 (2), 949–959.
- (28) Wulfers, M. J.; Tzolova-Müller, G.; Villegas, J. I.; Murzin, D. Y.; Jentoft, F. C. Evolution of carbonaceous deposits on H-mordenite and Pt-doped H-mordenite during n-butane conversion. *J. Catal.* **2012**, 296, 132–142.
- (29) Dong, J.; Zhang, K.; Li, X.; Qian, Y.; Zhu, H.; Yuan, D.; Xu, Q.-H.; Jiang, J.; Zhao, D. Ultrathin two-dimensional porous organic nanosheets with molecular rotors for chemical sensing. *Nat. Commun.* **2017**, *8* (1), No. 1142.
- (30) Michorczyk, P.; Wegrzyniak, A.; Wegrzynowicz, A.; Handzlik, J. Simple and efficient way of molybdenum oxide-based catalyst activation for olefins metathesis by methane pretreatment. *ACS Catal.* **2019**, 9 (12), 11461–11467.
- (31) Seman, M.; Kondo, J.; Domen, K.; Radhakrishnan, R.; Oyama, S. Reactive and inert surface species observed during methanol oxidation over silica-supported molybdenum oxide. *J. Phys. Chem. B* **2002**, *106* (50), 12965–12977.
- (32) Ghosh, A. K.; Kydd, R. A. A Fourier-transform infrared spectral study of propene reactions on acidic zeolites. *J. Catal.* **1986**, *100* (1), 185–195.
- (33) Gabrienko, A. A.; Danilova, I. G.; Arzumanov, S. S.; Pirutko, L. V.; Freude, D.; Stepanov, A. G. Direct measurement of zeolite Brønsted acidity by FTIR spectroscopy: solid-state 1H MAS NMR approach for reliable determination of the integrated molar absorption coefficients. *J. Phys. Chem. B* **2018**, *122* (44), 25386–25395.
- (34) Solans-Monfort, X.; Coperet, C.; Eisenstein, O. Shutting Down Secondary Reaction Pathways: The Essential Role of the Pyrrolyl Ligand in Improving Silica Supported d0-ML4 Alkene Metathesis Catalysts from DFT Calculations. *J. Am. Chem. Soc.* **2010**, *132* (22), 7750–7757.
- (35) Solans-Monfort, X.; Copéret, C.; Eisenstein, O. Oxo vs Imido Alkylidene d0-Metal Species: How and Why Do They Differ in Structure, Activity, and Efficiency in Alkene Metathesis? *Organometallics* **2012**, *31* (19), 6812–6822.
- (36) Grünert, W.; Stakheev, A. Y.; Feldhaus, R.; Anders, K.; Shpiro, E. S.; Minachev, K. M. Reduction and metathesis activity of MoO3/Al2O3 catalysts II. The activation of MoO3/Al2O3 catalysts. *J. Catal.* **1992**, *135* (1), 287–299.
- (37) Zhang, Q.; Xiao, T.; Liu, C.; Otroshchenko, T.; Kondratenko, E. V. Performance Descriptors for Catalysts Based on Molybdenum, Tungsten, or Rhenium Oxides for Metathesis of Ethylene with 2-Butenes to Propene. *Angew. Chem., Int. Ed.* **2023**, 62 (40), No. e202308872.
- (38) Chan, K. W.; Mance, D.; Safonova, O. V.; Copéret, C. Well-Defined Silica-Supported Tungsten(IV)—Oxo Complex: Olefin Metathesis Activity, Initiation, and Role of Brønsted Acid Sites. J. Am. Chem. Soc. 2019, 141 (45), 18286—18292.

- (39) Chan, K. W.; Lam, E.; D'Anna, V.; Allouche, F.; Michel, C.; Safonova, O. V.; Sautet, P.; Copéret, C. C—H Activation and Proton Transfer Initiate Alkene Metathesis Activity of the Tungsten(IV)—Oxo Complex. J. Am. Chem. Soc. 2018, 140 (36), 11395—11401.
- (40) Freundlich, J. S.; Schrock, R. R.; Cummins, C. C.; Davis, W. M. Organometallic Complexes of Tantalum That Contain the Triamido-amine Ligand, [(Me3SiNCH2CH2) 3N] 3-, Including an Ethylidene Complex Formed via a Phosphine-Catalyzed Rearrangement of an Ethylene Complex. J. Am. Chem. Soc. 1994, 116 (14), 6476–6477.
- (41) Hirsekorn, K. F.; Veige, A. S.; Marshak, M. P.; Koldobskaya, Y.; Wolczanski, P. T.; Cundari, T. R.; Lobkovsky, E. B. Thermodynamics, Kinetics, and Mechanism of (silox) 3M (olefin) to (silox) 3M (alkylidene) Rearrangements (silox= tBu3SiO; M= Nb, Ta). *J. Am. Chem. Soc.* **2005**, 127 (13), 4809–4830.
- (42) Liu, S.; Schrock, R. R.; Conley, M. P.; Tsay, C.; Carta, V. An Exploration of the Acid-Catalyzed Interconversion of Mo (NAr)-(CR1R2)(OR) 2 Complexes and Their Mo (NAr)(Olefin)(OR) 2 Isomers (Ar= 2, 6-i-Pr2C6H3, OR= OSiPh3 or OAr). Organometallics 2023, 42 (16), 2251–2261.
- (43) Liu, S.; Conley, M. P.; Schrock, R. R. Synthesis of Mo(IV) para-Substituted Styrene Complexes and an Exploration of Their Conversion to 1-Phenethylidene Complexes. *Organometallics* **2023**, 42 (11), 1087–1093.
- (44) Handzlik, J.; Kurleto, K.; Gierada, M. Computational Insights into Active Site Formation during Alkene Metathesis over a MoO x/SiO2 Catalyst: The Role of Surface Silanols. *ACS Catal.* **2021**, *11* (21), 13575–13590.
- (45) Mazoyer, E.; Szeto, K. C.; Norsic, S.; Garron, A.; Basset, J.-M.; Nicholas, C. P.; Taoufik, M. Production of propylene from 1-butene on highly active "bi-functional single active site" catalyst: tungsten carbene-hydride supported on alumina. *ACS Catal.* **2011**, *1* (12), 1643–1646.
- (46) Cho, H.-G.; Andrews, L. Infrared Spectra of CH3– MoH, CH2MoH2, and CH: MoH3 Formed by Activation of CH4 by Molybdenum Atoms. *J. Am. Chem. Soc.* **2005**, *127* (22), 8226–8231. (47) Schnieders, D.; Tsui, B. T.; Sung, M. M.; Bortolus, M. R.; Schrobilgen, G. J.; Neugebauer, J.; Morris, R. H. Metal hydride vibrations: The trans effect of the hydride. *Inorg. Chem.* **2019**, *58* (18), 12467–12479.



CAS BIOFINDER DISCOVERY PLATFORM™

STOP DIGGING THROUGH DATA —START MAKING DISCOVERIES

CAS BioFinder helps you find the right biological insights in seconds

Start your search

